Reference Switching Impulse Voltage Measuring System Based on Correcting the Voltage Divider Response With Software

Jussi Havunen and Jari Hällström

***Abstract*— The performance of a high-voltage switching impulse (SI) measurement system is highly dependent on the characteristics of the used voltage divider. Self-built or commercial voltage dividers do not always fulfill the requirements set for reference-level devices. Software corrections to improve the non-ideal divider response are easy to implement. This article describes the traceability and performance of the SI measurement systems of VTT MIKES up to 400 kV. Traceability is based on a calculable impulse voltage calibrator, which is used for calibration of a reference digitizer and a 10-kV divider. The 10-kV divider is then used to calibrate the 400-kV modular divider. Responses of both dividers are corrected using two different software methods. Implementation of these software methods allows state-of-the-art impulse parameter uncertainties. The most significant uncertainty component of time to peak is related to its definition and evaluation according to IEC 60060-1:2010 and IEC 61083–2:2013.**

***Index Terms*— Error correction, high-voltage techniques, impulse testing, measurement techniques, measurement uncertainty.**

I. Introduction

IMPULSE voltages are used for dielectric tests of high-voltage equipment. By definition, the impulse voltage is intentionally generated aperiodic transient voltage, which rapidly reaches its peak value and then falls slowly to zero. The impulse voltage with longer than 20-μs front time is called a switching impulse (SI), whereas the lightning impulse (LI) has a front time of less than 20 μs [1]. SI voltages are applied to test objects in order to simulate the voltage stress caused by a switching event in a supply network. Amplitudes of the SI voltages during testing are usually tens or hundreds of kilovolts.

According to IEC 60060-1:2010, the SI voltage has three main parameters: peak voltage U_p, time to peak T_p, and time to half-value T_2. U_p describes the maximum value of the impulse voltage, T_p is the time interval from the beginning of the impulse to the time of the maximum value of the impulse, and T_2 is the time interval from the beginning of the impulse to the time where the voltage has first decreased to half the maximum value. The standard SI voltage has T_p of 250 μs $\pm$ 20% and T_2 of 2500 μs $\pm$ 60% [1].

Manuscript received August 18, 2020; revised January 29, 2021; accepted February 18, 2021. Date of publication March 4, 2021; date of current version March 22, 2021. The Associate Editor coordinating the review process was Ron Goldfarb. *(Corresponding author: Jussi Havunen.)*

The authors are with the National Metrology Institute VTT MIKES, VTT Technical Research Centre of Finland, Espoo 02044, Finland (e-mail: jussi.havunen@vtt.fi).

Digital Object Identifier 10.1109/TIM.2021.3063753

Impulse voltages are usually measured with a system consisting of a voltage divider with a possible damping resistor, a signal cable, and a digitizer (transient recorder) with a possible attenuator. The damping resistor is used to attenuate unwanted transients from the impulse. The voltage divider is used to convert the high-voltage impulse to a low-voltage impulse, maintaining the impulse shape. The signal cable is used to transmit the low-voltage signal to the input of the digitizer. An additional attenuator can be used if the signal is too high for the digitizer input. An approved measuring system for SI voltage should be periodically calibrated, and it should be able to measure the peak value with less than 3% and the time parameters with less than 10% expanded uncertainty ($k = 2$) [2]. Currently, National Metrology Institutes (NMIs) can provide expanded uncertainties ($k = 2$) as low as 0.1% for U_p, 2% for T_p, and 1% for T_2 with standard SI voltages up to 100 kV and with higher uncertainty up to 1500 kV [3].

The performance of a measuring system is highly dependent on the performance of the used voltage divider. Voltage dividers used with SI need to withstand high voltages while having good dynamic properties. SI dividers do not need to have as high bandwidth as LI dividers, but they need to have a proper response up to some milliseconds. A good voltage divider does not distort the signal, i.e., time parameters of the output voltage of the divider correspond to the actual high-voltage impulse. SI voltages are usually measured with damped-capacitive voltage dividers (Zaengl type) [4] since resistive dividers have challenges to withstand the impulse energy [5].

Designing and building a reference-level damped capacitive voltage divider for impulse voltage measurements are not trivial [5], [6]. Price and available parts might limit the development so that the best available performance is not achieved. If the performance of the developed divider does not match the required performance, then the divider should be replaced or improved. Purchasing or manufacturing a new divider might be expensive, and hardware improvements can be very hard to implement since the design and used components are often fixed. Nevertheless, software corrections can be easily applied to correct the known errors of the divider output voltage [7].

This study presents the SI measurement capabilities of VTT MIKES up to 400 kV, extending the proceedings paper [7]. The low time parameter uncertainty is achieved due to the software-corrected divider response. The basis of the traceability is a calculable impulse voltage calibrator [8] together with a mercury-wetted relay-based step voltage generator. The

impulse calibrator is used to evaluate the performance of the reference digitizer and the 10-kV voltage divider. The drooping response of the-10 kV damped capacitive reference divider–originally designed for LI use is corrected using its known *RC* time constant in the time domain [7]. The 10-kV divider-based system can then be used to verify the performance of a system based on a modular 400-kV voltage divider. The step response of the 400-kV divider is corrected with software in the frequency domain using deconvolution [7].

II. Calculable Impulse Voltage Calibrator

The calculable impulse voltage calibrator [8] generates standard SIs according to IEC 60060-1:2010. U_p, T_p, and T_2 of the generated impulses are calculated from the component values of the impulse forming network. This network consists of the generation circuit and the input impedance of the system under calibration. Impulses can be generated from 50 mV to 300 V into high-impedance load.

Basically, the calibrator is a single-stage impulse generator where all the component values are known. The calibrator output is connected to the input of the system under calibration, i.e., a digitizer or a system consisting of an impulse divider (attenuator) and a digitizer. Input resistance and capacitance of the system under calibration are measured, and they are used for the evaluation of the reference impulse parameters. Time parameters are only dependent on the component values but also the charging voltage needs to be measured with a voltmeter in order to calculate U_p. Parameters measured by the system under calibration are then compared to the reference values.

The used calculable impulse voltage calibrator provides a traceable method for impulse parameter calibration up to 300 V. Expanded uncertainty ($k = 2$) of the calibrator is 0.14% for U_p, 0.36% for T_p, and 0.28% for T_2 [8]. This calibrator is the basis of the traceability chain of the impulse measuring systems used at VTT MIKES, and it is used to characterize both the reference digitizer discussed in Section III and a damped capacitive voltage divider-based system discussed in Section IV.

III. Digitizer and Evaluation Software

A commercial 12-bit digitizer with good step response [9] is used as a transient recorder in SI voltage measurements. Two input channels allow measurements of two voltage divider outputs simultaneously. Impulses up to 10 V can be directly measured using this digitizer.

A self-made evaluation algorithm fits a double-exponential function to the impulse data from 85% on the front to 95% on the tail for T_p calculation [10]. Impulse data are filtered in order to reduce the unwanted effect of noise to T_2 calculation.

A. Digitizer Performance

The 10-MS/s sampling rate is used for SI voltage measurement. Digitizer gain corrections are used for each digitizer range. All gain corrections are less than 0.2%, and they are based on the measurements performed with the calculable impulse voltage calibrator. The temperature dependence of the digitizer ranges is also corrected. The measured temperature coefficient is approximately 0.05%/°C, which is in line with the manufacturer's specifications. Calibration results for digitizers are presented in Fig. 1. U_p was set to 90% of the effective range.

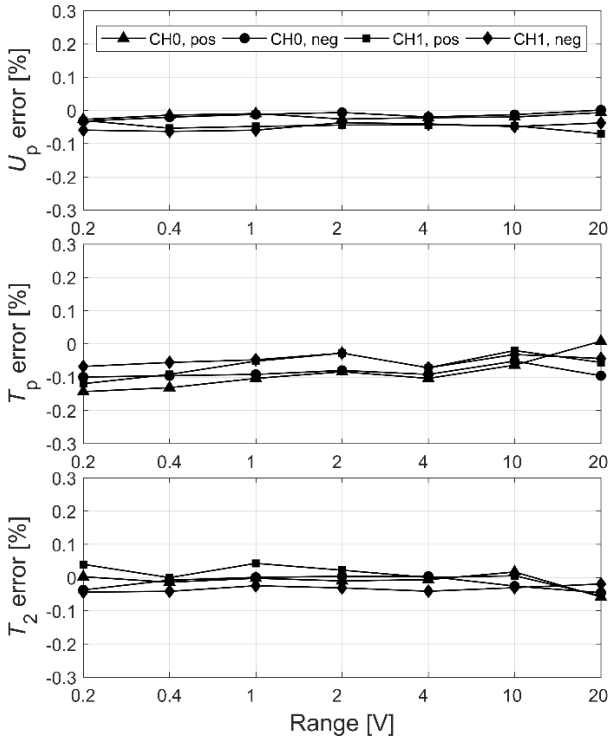

Fig. 1. SI calibration results of the digitizer with 250-/2500-μs impulses. Calibrator uncertainty ($k = 2$) is 0.14% for U_p, 0.36% for T_p, and 0.28% for T_2.

All calibration errors are less than half of the calibrator uncertainty. The linearity of the digitizer ranges has been tested with lower impulse voltage, i.e., U_p was set to 40% of the effective range. The observed nonlinearity is well within the uncertainty of the used calibrator. The long-term stability has been verified by comparing the results from the last two calibrations when the calibration interval is 12 months. Changes in all parameters were $\leq$0.04%. The performance of the digitizer is sufficient for reference use. Both channels show similar behavior so that they can be interchanged with the used voltage dividers.

B. Software Performance

Evaluation software has been verified using the test data generator (TDG) of IEC 61083-2 [11]. TDG currently has five different waveforms for SI voltages: three analytic (A) and two measured (M) impulses. Reference impulses were generated with 12-bit and 10-MS/s settings to correspond to the used digitizer. No additional noise was added to the data. TDG results are presented in Table I. Software performance fulfills the acceptance limits given in the standard.

Clause 5.9 of IEC 60060-2 [2] specifies software effect as one uncertainty component. According to Annex B of IEC 61083-2 [11], the standard uncertainty ($k = 1$) for software,

TABLE I
TDG RESULTS

Impulse	U_p difference	T_p difference	T_2 difference
SI-A1	0.04 %	0.36 %	0.06 %
SI-A2	0.00 %	1.01 %	0.00 %
SI-A3	0.00 %	0.46 %	-0.01 %
SI-M1	0.09 %	1.55 %	0.15 %
SI-M2	-0.06 %	2.52 %	0.96 %

TABLE II
COMPARISON OF UNCERTAINTIES

	Expanded uncertainty ($k = 2$) U_p	T_p	T_2
The best NMI capabilities at 100 kV	0.10 %	2.00 %	1.00 %
IEC 61083-2 reference for SI, u_{B72}	0.13 %	4.00 %	2.00 %
VTT MIKES software uncertainty			
with A1-A3, u_{B7_A}	0.04 %	2.32 %	0.06 %
with A1-A3, M1-M2, u_{B7_B}	0.16 %	4.94 %	2.28 %
10 kV system without u_{B7}	0.19 %	0.48 %	0.34 %
10 kV system with u_{B7_A}	0.19 %	2.37 %	0.35 %
10 kV system with u_{B7_B}	0.25 %	4.96 %	2.31 %
400 kV system without u_{B7}	0.20 %	0.55 %	0.03 %
400 kV system with u_{B7_A}	0.21 %	2.38 %	0.41 %
400 kV system with u_{B7_B}	0.26 %	4.97 %	2.32 %
VTT MIKES CMCs (up to 200 kV)	0.20 %	3.00 %	1.00 %

u_{B7}, is calculated as

$$u_{B7} = \sqrt{u_{B71}^2 + u_{B72}^2} \tag{1}$$

where u_{B71} is the maximum observed difference for a parameter divided with $\sqrt{3}$, and u_{B72} is the standard uncertainty of the reference value defined in IEC 61083-2. By using all the SI waveforms and applying only u_{B72}, the smallest possible software uncertainties can be achieved. In Table II, these uncertainties are compared to the best NMI uncertainties. The best NMI level uncertainties [3] are not possible at the system level if they refer to IEC 60060-2 and 61083-2 standards in their uncertainty evaluation.

Measured waveforms M1–M2 of TDG do not present impulses used for calibration purposes because of the wave shape or excessive noise. Therefore, it is justified to use just the analytic waveforms A1–A3 in the uncertainty evaluation. Expanded uncertainty ($k = 2$) of the VTT MIKES evaluation software using the analytic waveforms (u_{B7_A}) or all waveforms (u_{B7_B}) are presented in Table II.

IV. 10-kV MEASURING SYSTEM

The 10-kV measuring system consists of a coaxial damped-capacitive divider and the digitizer presented in Section III. The peak voltage is limited to 10 kV by the used input connector of the divider. The divider 100-pF high-voltage arm consists of two NPO type ceramic capacitors in parallel, each with an 82-Ω damping resistor, which leads to c. 8-ns time constant. It is used with two different low-voltage arms

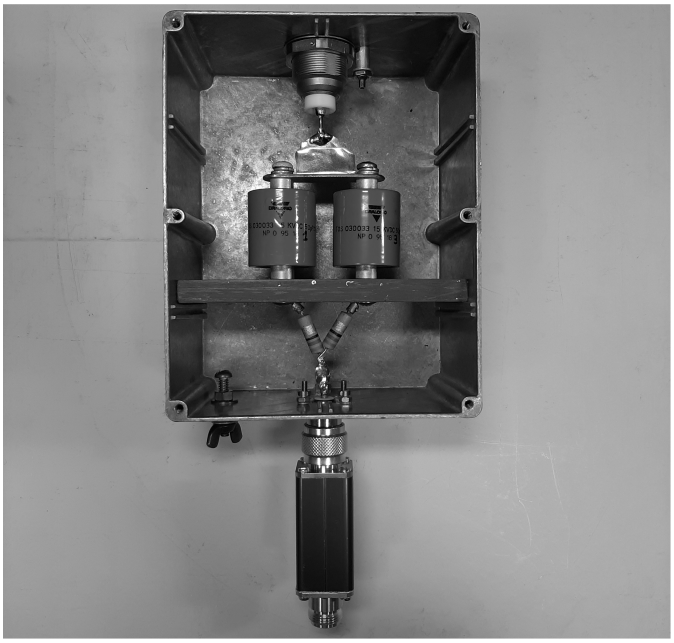

Fig. 2. Structure of the 10-kV damped-capacitive voltage divider. The coaxially built low-voltage arm is connected to the high-voltage arm using an N-connector.

with 18.8- and 132-nF nominal capacitances having their time constants matched with the high-voltage arm. Because of the very low time constant, these damping resistors are ignored in the following analysis. Divider scale factors are 184.6 and 1308, respectively. The used digitizer has a 10-V maximum input, and the 18.8-nF low-voltage arm allows measurements up to 1.8 kV and 132 nF up to 10 kV. A 50-Ω series matching resistor is used at the divider end of the 100-cm measuring cable to absorb the reflection arriving from the digitizer end of the cable.

Since the discharge time constant of the low-voltage arm (18.8 nF) together with digitizer 1-MΩ input has originally been designed only for (LI) voltage measurements, the divider cannot be used for SI measurements without improvements. With the 1-MΩ digitizer input resistance, the calculated time constants for the two low-voltage arms are 18.63 and 131.72 ms, respectively. Nevertheless, the components used in the divider can withstand the increased impulse energy. The divider structure is presented in Fig. 2.

A. Initial Dynamic Performance

The time constant of the divider with an 18.8-nF low-voltage arm was evaluated from the measured step response in Fig. 3. This drooping response causes major errors in SI time parameters, especially on T_2. With the 132-nF low-voltage arm, the step response is better due to the longer time constant.

The initial performance of the system was verified at 300 V with nominal SI using both low-voltage arms. Calibration results are presented in Table III.

B. Droop Correction of Divider Response

The drooping step response occurs when the capacitance of the low-voltage arm, C_{low}, discharges through the parallel

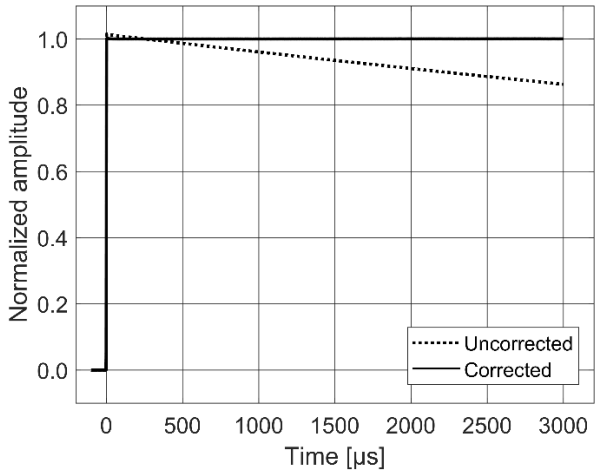

Fig. 3. Step response of the 10-kV divider used with the 18.8-nF low-voltage arm before and after correction. Step responses are normalized to the 250-μs level.

TABLE III
PERFORMANCE OF THE MEASURING SYSTEMS

	Difference to reference		
	U_p	T_p	T_2
10 kV measuring system, 18.8 nF low-voltage arm, initial	-1.1 %	-4.1 %	-19 %
10 kV measuring system, 132 nF low-voltage arm, initial	-0.2 %	-0.6 %	-3.3 %
10 kV measuring system, 18.8 nF low-voltage arm, corrected	0.03 %	-0.06 %	0.04 %
10 kV measuring system, 132 nF low-voltage arm, corrected	0.03 %	-0.04 %	0.02 %
140 kV measuring system, initial	0.6 %	0.7 %	-0.1 %
140 kV measuring system, corrected	0.00 %	-0.10 %	-0.10 %
400 kV measuring system, corrected	0.00 %	-0.09 %	-0.08 %

input resistance R_{in} with a time constant τ

$$\tau = R_{\text{in}} \cdot C_{\text{low}}. \tag{2}$$

In addition to the low-voltage arm capacitance, C_{low} also includes the capacitance of the used measuring cable and the input capacitance of the used digitizer or attenuator. The input resistance of the used digitizer or attenuator dominates R_{in}. R_{in} and C_{low} of the two low-voltage arms are measured using an *LCR* meter.

The first-order decay of the divider low-voltage arm can be modeled by

$$U_o(\omega) = \frac{1}{sf} \cdot \frac{j\omega}{j\omega + \omega_c} U_i(\omega) \tag{3}$$

TABLE IV
CALIBRATION RESULTS USING THE 18.8-nF LOW-VOLTAGE ARM

Digitizer CH0 range	U_p reference value	U_p error	T_p error	T_2 error
4 V	-300 V	0.01 %	-0.09 %	0.03 %
2 V	-300 V	0.04 %	-0.02 %	0.06 %
1 V	-166 V	0.05 %	-0.04 %	0.04 %
0.4 V	-66 V	0.05 %	-0.07 %	0.03 %
0.2 V	-33 V	0.01 %	-0.09 %	0.03 %
0.2 V	33 V	0.02 %	-0.09 %	0.04 %
0.4 V	66 V	0.04 %	-0.06 %	0.04 %
1 V	166 V	0.04 %	-0.07 %	0.07 %
2 V	300 V	0.02 %	-0.01 %	0.03 %
4 V	300 V	0.04 %	-0.10 %	0.02 %
	average	0.03 %	-0.06 %	0.04 %
	stdev	0.02 %	0.03 %	0.02 %

where U_i and U_o are the input and output voltages of the divider, sf is the divider scale factor, and $\omega_c = 1/\tau$. The corresponding inverse filtering is performed by

$$U_i(\omega) = sf \cdot \left[1 + \frac{\omega_c}{j\omega} U_o(\omega)\right] \tag{4}$$

and it can be represented in the time domain by

$$U_i(t) = sf \cdot \left[U_o(t) + \omega_c \int_0^t U_o(t)dt\right]. \tag{5}$$

If the time constant is known, the corrected signal can be derived from the measured data. This time domain-based correction has successfully been applied to correct the output of a charge amplifier in low-level partial discharge measurements [12] and to correct the response of this 10-kV SI voltage divider [7]. Time-based correction is easy to implement in software.

C. Performance After Correction

The validity of the correction was visually verified by measuring the step response of the divider using the correction (see Fig. 3). Improved step response indicates better performance.

The 10-kV measuring system was calibrated with the calculable impulse voltage calibrator. Reference time parameters were $T_p = 256$ μs and $T_2 = 2666$ μs. The result for the 18.8-nF low-voltage arm are presented in Table IV and for 132 nF in Table V. All errors are within the uncertainty limits of the calibrator, which indicates that the correction was successful. Corrected calibration results are compared to the initial results in Table III. The same scale factors were used with the initial and corrected results.

D. Uncertainty Budget

Uncertainty of the 10-kV measuring system was evaluated based on the components presented in IEC 60060-2:2010 [2] according to principles set out in JCGM Guide 100 [13]. The same budget was used for both low-voltage arms since the differences in impulse calibrations were minor. The uncertainty budget is presented in Table VI. *Reference* uncertainty is the uncertainty of the impulse calibrator.

TABLE V
CALIBRATION RESULTS USING THE 132-nF LOW-VOLTAGE ARM

Digitizer CH0 range	U_p reference value	U_p error	T_p error	T_2 error
0.4 V	-300 V	0.05 %	-0.02 %	-0.04 %
0.2 V	-235 V	0.01 %	-0.05 %	0.04 %
0.2 V	235 V	0.01 %	-0.06 %	0.03 %
0.4 V	300 V	0.04 %	-0.02 %	0.05 %
	average	0.03 %	-0.04 %	0.02 %
	stdev	0.02 %	0.02 %	0.04 %

TABLE VI
UNCERTAINTY BUDGET FOR THE 10-kV MEASURING SYSTEM

Source	Contribution to standard uncertainty ($k = 1$)		
	U_p	T_p	T_2
Reference	0.07 %	0.18 %	0.14 %
Average error	0.02 %	-0.06 %	0.03 %
u_{B0}	0.02 %	0.03 %	0.04 %
u_{B1}	0.01 %	-	-
u_{B2}	0.03 %	0.14 %	0.06 %
u_{B3}	0.01 %	-	-
u_{B4}	0.05 %	0.02 %	0.06 %
u_{B5}	-0.03 %	-0.01 %	-0.01 %
u_{B6}	-	-	-
u_{B7}	0.02 %	1.16 %	0.03 %
Total standard uncertainty	0.10 %	1.18 %	0.17 %
Total expanded uncertainty ($k = 2$)	0.19 %	2.37 %	0.35 %

Average errors against the reference calibrator and *nonlinearity* u_{B0} were calculated according to Tables IV and V.

Linearity extension u_{B1} is based on the measured voltage dependence of the capacitance of the high- and low-voltage arms. Changes are in the same direction and less than 0.005% over the operating voltage range.

Dynamic behavior u_{B2} was tested using a 20/4000-μs impulse calibrator. $T_p = 20$ μs is out of the limits of a standard SI. With this time scale, the digitizer's nonideal step response was corrected using deconvolution [14].

The *short-term stability* u_{B3} has been tested by measuring the ac scale factor of the divider before and after applying a set of 11-kV impulses. No significant changes were observed in the scale factor.

The *long-term stability* u_{B4} is based on recalibration after six months at 300 V using both low-voltage arms when the calibration interval is 24 months.

The *ambient temperature effect* u_{B5} was determined by performing impulse calibration at 23 °C temperature and repeating the calibration after the divider had been several hours in a 30 °C temperature chamber. Results are scaled to show the effect of a 5 °C difference. The 132-nF low-voltage arm was more sensitive to temperature, and its results are taken into account.

The *proximity effect* u_{B6} is not applicable since the divider is a closed coaxial structure.

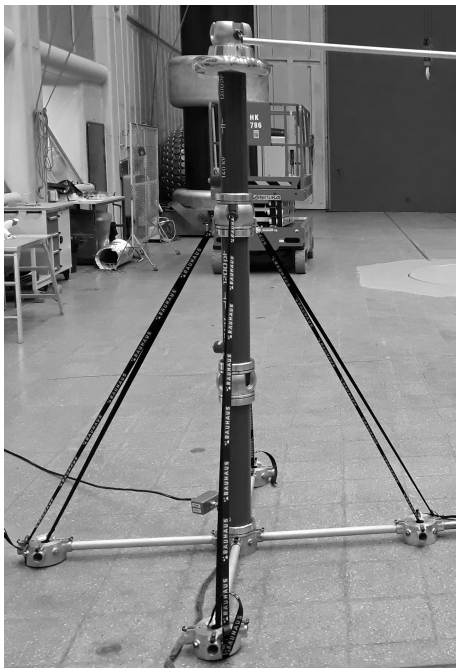

Fig. 4. Modular 400-kV damped-capacitive voltage divider. The high-voltage arm consists of three 1200-pF modules and a fixed high-voltage lead with a 200-Ω damping resistor. A 15-m cable with an attenuator is used with the 400-nF low-voltage arm.

The *software effect* u_{B7} is based on the TDG SI waveforms A1−A3 (u_{B7_A}).

Expanded uncertainties ($k = 2$) with and without the software uncertainties are summarized in Table II. Most uncertainty components are smaller than the uncertainty of the reference calibrator. Results show that the most dominating uncertainty component for T_p is the software uncertainty if it is taken into account. It is justified to neglect the software uncertainty when using smooth double-exponential waveshapes since the traceability of the used reference is tied to the definition of T_p, not to its calculation. IEC 60060-1 is currently under revision, which might improve the definition of T_p and the uncertainties related to the software.

V. 400-kV MEASURING SYSTEM

The 400-kV measuring system consists of a modular damped-capacitive voltage divider and the digitizer presented in Section III. The modular structure makes the divider ideal for on-site calibrations. The divider can be used with one to three high-voltage modules, each having a 1200-pF capacitance value. Each paper–oil capacitor module has a nominal peak voltage of 140 kV. The low-voltage arm has a nominal capacitance of 400 nF and has a 50-Ω series matching resistor for the cable. A 200-Ω damping resistor is used in a fixed high-voltage lead to dampen possible transients. The 15-m cable with an additional high-impedance impulse attenuator (52:1) delivers the signal to the digitizer input. The scale factor is 54 500 when used with three modules and the attenuator. The divider is shown in Fig. 4.

A. Initial Performance

The distorted step response of a single-module voltage divider is presented in Fig. 5. All three high-voltage modules

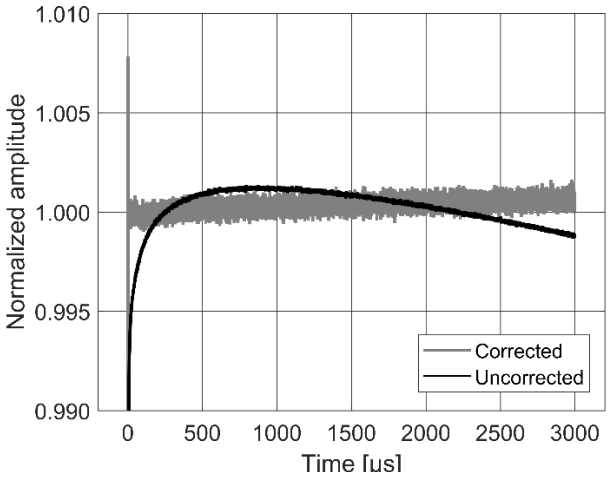

Fig. 5. Step response of a single-module divider (140 kV) used with the 400-nF low-voltage arm before and after correction. Step responses are normalized to the 250-μs level.

have almost identical step responses, and similar results were obtained using two or three modules in series. Even though large dividers are often sensitive to the measurement circuit [15], no significant proximity effects were found in this case due to the relatively large capacitance of the divider.

The voltage divider was calibrated by comparison with the 10-kV reference system. Two-channel measurements allow us to use the same digitizer in both measuring systems. The initial performance of a divider consisting of a single 140-kV module is shown in Table III.

The used impulse attenuator was also characterized separately using the calculable impulse voltage calibrator. With standard SI, it showed errors $\leq 0.1\%$ for time parameters. This means that the influence of the attenuator is negligible in the voltage divider response. Nonetheless, the attenuator was included in the step response measurement and treated as a part of the voltage divider.

B. Step response Correction for Divider

While the step response reveals the nonideal dynamic properties of the divider, its time derivative (impulse response) can be applied to correct the nonidealities of the divider. In general, impulse response $g(t)$ of an instrument and a mathematical process called deconvolution can be used to reverse the known effects of the instrument on the measured signal [16]. Deconvolution-based methods have been reported to correct the dynamic behavior of digitizers and large dividers used with LI voltage measurements [14], [15], [17]. Since LI is shorter in duration, it requires higher bandwidth and sampling rate, which can cause noise-related problems to the correction [17]. Therefore, it is very tempting to use this correction to SI measurements without the need for any additional filtering. However, in this case, the used parameter evaluation applies a filter to improve the evaluation of T_2.

The step response of the divider was determined by applying a voltage step $u_i(t)$ to its input and by measuring the output voltage $u_o(t)$ with a digitizer. The used step voltage generator is based on the mercury-wetted relay, and it shorts applied voltage to the ground. The 300-V voltage step was used in this case, and 100 steps were averaged to reduce the noise level. A single 1200-pF high-voltage module was used together with the damping resistor, low-voltage arm, 15-m cable, and the 52:1 attenuator. The output signal was too small to be measured with the digitizer presented in Section II, so it was measured with an additional digitizer with more suitable input ranges. Digitizer's response was not corrected, but its influence was estimated to be negligible.

The impulse response, $g(t)$, can be converted to frequency response $G(\mathrm{s})$. Conversions between the time and frequency domains are performed using the fast Fourier transform (FFT) and the inverse FFT (IFFT). $G(\mathrm{s})$ ties the instrument's input voltage $U_i(\mathrm{s})$ and the output voltage $U_o(\mathrm{s})$ in the following way in the frequency domain:

$$G(s) = \frac{U_o(s)}{U_i(s)}. \tag{6}$$

When the output voltage $U_o(\mathrm{s})$ and the frequency response $G(\mathrm{s})$ are known, we can use them to define the input voltage $U_i(\mathrm{s})$

$$U_i(s) = \frac{U_o(s)}{G(s)}. \tag{7}$$

This process is called deconvolution. It can be applied to impulse measurements so that the applied impulse is used as $u_i(t)$ and the instrument's impulse response as $g(t)$.

The deconvolution-based step response correction has been implemented in measurement software, and it successfully corrected the response of a 140-kV SI divider [7]. In this study, a similar correction is used also for this modular divider consisting of two or three similar high-voltage modules.

C. Performance After Correction

The validity of the correction was visually verified by measuring the step response again by using the correction. The step response rises now much faster and is flatter, which indicates improved performance (see Fig. 5). However, deconvolution increased the noise level slightly, which can cause additional errors on small-signal levels. Additional filtering for the signal was not used even though it might be necessary for LI measurements [17] where higher sample rate and bandwidth are applied.

The modular divider was calibrated against the 10-kV divider presented in Section IV. Both low-voltage arms were used with the reference divider, marked as 1.8 and 10 kV according to their maximum voltage. During the calibration, U_p was from 300 V to 10 kV, T_p from 214 to 267 μs, and T_2 from 1982 to 2124 μs. Calibration results are presented in Table VII and compared to other systems in Table III.

Calibration was also performed without the 52:1 attenuator in order to see if the deconvolution-based correction is dependent on signal level. It was noted that, when U_p was approximately 25% of the smallest digitizer range, it caused a circa -0.2% difference to both time parameters compared to the results obtained with higher voltage levels. This is probably caused by the noise introduced during the deconvolution process.

TABLE VII
CALIBRATION RESULTS FOR THE MODULAR DIVIDER

Ref.	Modules	52:1 attn.	U_p [kV]	U_p error	T_p error	T_2 error
1.8 kV	1	no	-0.99	0.01 %	-0.04 %	-0.05 %
1.8 kV	1	no	-1.25	-0.02 %	-0.04 %	-0.11 %
10 kV	1	no	-1.01	-0.01 %	-0.02 %	-0.04 %
10 kV	1	no	-3.00	0.01 %	-0.04 %	-0.01 %
10 kV	1	yes	-1.01	0.00 %	-0.35 %	-0.27 %
10 kV	1	yes	-1.61	-0.01 %	-0.21 %	-0.16 %
10 kV	1	yes	-3.05	0.01 %	-0.09 %	-0.05 %
10 kV	1	yes	-4.69	0.00 %	-0.02 %	-0.10 %
10 kV	1	yes	-9.54	-0.01 %	-0.10 %	-0.11 %
1.8 kV	2	no	-1.17	0.01 %	0.00 %	-0.01 %
10 kV	2	no	-6.09	-0.01 %	-0.02 %	-0.01 %
10 kV	2	yes	-6.00	0.00 %	-0.06 %	-0.12 %
1.8 kV	3	no	-0.32	0.00 %	-0.08 %	-0.06 %
1.8 kV	3	no	-0.84	0.01 %	-0.07 %	-0.02 %
10 kV	3	no	-8.82	0.00 %	-0.08 %	-0.06 %
10 kV	3	yes	-9.63	0.00 %	-0.15 %	-0.04 %
		average		0.00 %	-0.09 %	0.08 %
		stdev		0.01 %	0.09 %	0.07 %

TABLE VIII
UNCERTAINTY BUDGET FOR THE 400-kV MEASURING SYSTEM

Source	Contribution to standard uncertainty ($k = 1$) U_p	T_p	T_2
Reference	0.10 %	0.24 %	0.17 %
Average error	0.00 %	-0.09 %	-0.08 %
u_{B0}	0.01 %	0.05 %	0.04 %
u_{B1}	0.02 %	-	-
u_{B2}	-	0.06 %	-0.04 %
u_{B3}	0.02 %	-	-
u_{B4}	-	0.02 %	0.04 %
u_{B5}	-	0.08%	-0.01 %
u_{B6}	-	0.00 %	0.00 %
u_{B7}	0.02 %	1.16 %	0.03 %
Total standard uncertainty	0.10 %	1.19 %	0.20 %
Total expanded uncertainty ($k = 2$)	0.21 %	2.38 %	0.41 %

D. Uncertainty Budget

Uncertainty of the modular 400-kV measuring system was evaluated based on the components presented in IEC 60060-2:2010 [2]. The same budget is used for all systems consisting of either one, two, or three modules. This uncertainty budget is presented in Table VIII.

Reference uncertainty is based on the uncertainty of the 10-kV reference measuring system without the software uncertainty u_{B7}. Software uncertainty was excluded since both systems use the same evaluation, and this uncertainty is taken into account on both systems' uncertainty budgets separately.

Average errors against the reference system and *nonlinearity* u_{B0} were calculated according to Table VII.

Linearity extension u_{B1} is based on the LI scale factor measurement of each module at 50, 90, and 140 kV against a LI reference system [14], [18].

Dynamic behavior u_{B2} was tested against the 10-kV reference divider using 20-/4000-μs SI from the calibrator.

The *short-term stability* u_{B3} was tested by applying ten 140-kV LI impulses separately to all modules and checking how much the scale factors changed during the test.

Since the scale factor of the system is highly dependent on the used ambient conditions, it is always calibrated against the 10-kV system before and after its use. Therefore, the *long-term stability* u_{B4} and the *temperature effect* u_{B5} can be neglected for U_p. The long-term stability of the time parameters is based on two calibrations performed within five months when the calibration interval is two years. The temperature effect for time parameters was measured at 20 °C and 23 °C, and it was scaled to show an uncertainty of 5 °C difference.

The *proximity effect* u_{B6} was tested by placing the divider 1 and 0.2 divider height from a grounded wall to test the effect to the time parameters. No measurable effects were found. Also, the divider is always calibrated using an impulse calibrator and 10-kV divider in the setup where the divider is used.

The *software effect* u_{B7} is based on the TDG SI waveforms A1−A3 (u_{B7_A}).

Most uncertainty components are smaller than the uncertainty of the reference system. As with the 10-kV divider, the most dominating uncertainty component for T_p is the software uncertainty, which can be neglected if smooth double-exponential waveshapes are used. Table II shows that the uncertainty of this system agrees, even with the software uncertainty u_{B7_A} included, with the current calibration and measurement capabilities (CMCs) of VTT MIKES [3] but extends the voltage range from 200 to 400 kV. However, the uncertainty estimate on higher voltages is waiting for validation in a suitable comparison.

VI. CONCLUSION

Two software-based methods for improvement of the performance of a SI voltage measuring system are demonstrated. The first-order drooping response of a 10-kV damped capacitive divider was corrected with a simple digital filter. Higher order correction for the 400-kV divider was performed using deconvolution. The introduction of these software corrections reduced the systematic time parameter errors from several percent to below 0.1%. Application of the corrections enabled state-of-the-art performance also for time parameter measurement. The most significant remaining uncertainty component is related to the definition and evaluation of time to peak according to IEC 60060-1:2010 and IEC 61083-2:2013.

REFERENCES

[1] *High-Voltage Test Techniques—Part 1: General Definitions and Test Requirements*, Standard IEC 60060-1:2010, 2010.
[2] *High-Voltage Test Techniques—Part 2: Measuring Systems*, Standard IEC 60060-2:2010, 2010.
[3] Bureau International des Poids et Mesures. *Calibration and Measurement Capabilities (CMCs)*. Accessed: Jul. 31, 2020. [Online]. Available: https://www.bipm.org/kcdb/
[4] W. Zaengl, "Das messen hoher, rasch veränderlicher stossspannungen," Ph.D. dissertation, Dept. F. f. Maschinenw. u. Elektrotechnik, TH München, Munich, Germany, 1964.
[5] A. Bergman and J. Hällström, "Impulse dividers for dummies," in *Proc. Int. Symp. High Voltage Eng. (ISH)*. Rotterdam, The Netherlands: Millpress, Aug. 2003, pp. 1–4.

[6] K. Schon, *High Impulse Voltage and Current Measurement Techniques: Fundamentals—Measuring Instruments—Measuring Methods*. Cham, Switzerland: Springer, 2013, pp. 142–151, doi: 10.1007/978-3-319-00378-8.

[7] J. Havunen and J. Hällström, "Software corrections for switching impulse voltage divider response," presented at the Conf. Precis. Electromagn. Meas. (CPEM), Aug. 2020.

[8] J. K. Hällström, Y. Y. Chekurov, and M. M. Aro, "A calculable impulse voltage calibrator for calibration of impulse digitizers," *IEEE Trans. Instrum. Meas.*, vol. 52, no. 2, pp. 400–403, Apr. 2003, doi: 10.1109/.TIM.2003.810714.

[9] A. Bergman, A.-P. Elg, and J. Hällström, "Evaluation of step response of transient recorders for lightning impulse," presented at the Int. Symp. High Voltage Eng. (ISH), 2017. Accessed: Jul. 31, 2020. [Online]. Available: https://e-cigre.org/publication/ISH2017_488-evaluation-of-step-response-of-transient-recorders-for-lightning-impulse

[10] A. Nilsson, A. Bergman, and J. Hällström, "An improved method for switching-impulse evaluation," in *Proc. Conf. Precis. Electromagn. Meas. (CPEM)*, Washington, DC, USA, Jul. 2012, pp. 20–21, doi: 10.1109/CPEM.2012.6250638.

[11] *Instruments and Software Used for Measurement in High-Voltage and High-Current Tests—Part 2: Requirements for Software for Tests With Impulse Voltages and Currents*, Standard IEC 61083-2:2013, 2013.

[12] J. Havunen and J. Hällström, "Application of charge-sensitive preamplifier for the calibration of partial discharge calibrators below 1 pC," *IEEE Trans. Instrum. Meas.*, vol. 68, no. 6, pp. 2034–2040, Jun. 2019, doi: 10.1109/TIM.2019.2895437.

[13] *Evaluation of Measurement Data—Guide to the Expression of Uncertainty in Measurement, (Joint Committee for Guides in Metrology, JCGM 100:2008)*. Accessed: Jan. 10, 2021. [Online]. Available: http://www.iso.org/sites/JCGM/GUM-introduction.htm

[14] J. Havunen, J. Hällström, A. Bergman, and A. E. Bergman, "Using deconvolution for correction of non-ideal step response of lightning impulsedigitizers and measurement systems," in *Proc. Int. Symp. High Voltage Eng. (ISH)*, 2017, pp. 1–6, doi: 10.5281/zenodo.3568022.

[15] W. Yan, W. Zhao, and Y. Li, "Effect of step response measurement arrangement on the correction of ultrahigh-voltage lightning impulse dividers," *IEEE Trans. Instrum. Meas.*, vol. 68, no. 6, pp. 1666–1670, Jun. 2019, doi: 10.1109/.TIM.2019.2900130.

[16] W. H. Press, S. A. Teukolsky, W. T. Vetterling, and B. P. Flannery, *Numerical Recipes in C++: The Art of Scientific Computing*, 2nd ed. Cambridge, U.K.: Cambridge Univ. Press, 2002, p. 1002.

[17] W. Zhao, J. Wang, C. Li, and H. Shao, "Study on the frequency bandwidth limits for deconvolution of the step response," in *Proc. Conf. Precis. Electromagn. Meas. (CPEM)*, Paris, France, Jul. 2018, pp. 1–2, doi: 10.1109/CPEM.2018.8501098.

[18] J. Hällström, J. Piiroinen, and M. Aro, "Design of shielded resistive reference divider for lightning impulses," in *Proc. Int. Symp. High Voltage Eng. (ISH)*, 1995, pp. 44–82.

Jussi Havunen was born in Laihia, Finland, in 1988. He received the B.Sc. and M.Sc. degrees in electrical engineering from the Tampere University of Technology (TUT), Tampere, Finland, in 2010 and 2013, respectively. He is currently pursuing the D.Sc. degree in measurement science with Aalto University, Espoo, Finland.

He was a Research Assistant and a part-time Teacher with TUT from 2011 to 2012, where he was working with the Superconductivity Research Group. From 2012 to 2013, he was a Trainee with ABB Drives, Helsinki, Finland, where his work was on modeling and measuring mechanical and electrical components of ac drives. He joined the National Metrology Institute VTT MIKES, VTT Technical Research Centre of Finland, Espoo, Finland, in 2014, where he is working with high-voltage metrology and calibrations.

Jari Hällström was born in Lappeenranta, Finland, in 1961. He received the M.Sc. and D.Sc. degrees in electrical engineering from the Helsinki University of Technology, Espoo, Finland, in 1987 and 2002, respectively.

Until 2008, he held various positions at the Helsinki University of Technology, where his first research interest was instrumentation for the measurement of magnetic fields of the human brain and later high-voltage metrology. Since 2008, he has been with the National Metrology Institute VTT MIKES, VTT Technical Research Centre of Finland, Espoo, where he is currently responsible for the Finnish National Standards for electrical power and high-voltage calibrations.

Dr. Hällström received the IEC 1906 Award for his work on the standardization of high-voltage measuring techniques in 2007.